

Electronic Supplementary Material (ESI) for ChemComm.
This journal is © The Royal Society of Chemistry 2015

Nitrogen-doped bamboo-like carbon nanotubes: promising anode materials for sodium-ion batteries

*Dongdong Li,^{ab‡} Lei Zhang,^{b‡} Hongbin Chen,^a Liang-xin Ding,^{*a} Suqing Wang^a and Haihui Wang^{*ab}*

^aSchool of Chemistry & Chemical Engineering, South China University of Technology,
Guangzhou, 510640, PR China.

^bSchool of Chemical Engineering, University of Adelaide, Adelaide, SA 5005, Australia

[‡]D. Li and L. Zhang contributed equally to this work.

S1.Experimental details

S1.1 Synthesis of N-BCNTs

N-BCNTs were prepared using a simple pyrolysis approach. Firstly, 5.0 g dicyandiamide (DCD) and 2.2 g cobaltous chloride hexahydrate were dispersed into deionised water (300 mL) via vigorous stirring. Then, the solution was put on a magnetic stirring heater with a controlled temperature of 100 °C and stirred until all the water was volatilised. Subsequently, the mixture was transferred to a tube furnace and annealed at 800 °C for 1 h in Ar. After that, the residuum was dissolved in HCl solution (2 M) for 24 h. Finally, the product was obtained after washing with deionised water and drying at 80 °C for 10 h.

S1.2 Physical characterization

N-BCNTs morphologies were determined using electron microscopy (SEM, Nova Nano 430) and transmission electron microscopy (TEM, JEM-2010). X-ray diffraction (XRD) was performed using a Bruker D8 Advance instrument and Cu Ka radiation. Raman spectra were recorded on an Aramis LabRam spectrometer using an excitation wavelength of 632.8 nm. X-ray photoelectron spectroscopy (XPS) was tested using an ESCALAB 250. An ASAP 2010 Micromeritics analyser (USA) was used to measure the nitrogen adsorption and desorption isotherms.

S1.3 Electrochemical test

All electrochemical tests conducted in this study utilised coin cells (CR2032). The coin cells were assembled on an argon-filled glove box. The working electrode was prepared in three steps. First, the slurry was prepared by mixing 80 wt% active materials, 10 wt% super P, and 10 wt% polyvinylidene (PVDF). Then, the slurry was casted on Cu foil. At last, the coated Cu foil was dried at 80 °C in a vacuum oven for 12 hours. The mass loading of N-BCNTs is around 1.2 mg cm⁻². Sodium metal

(Aladdin Industrial Corporation) was used as the counter electrode. A Whatman GF/D glass fibre was used as the separator. The electrolyte was 1 M NaClO₄ in ethylene (EC) and diethyl carbonate (DEC) (v:v=1:1) with 2 wt.% fluoroethylene carbonate (FEC) added. Electrochemical performances were tested between 0.01 and 3.0 V using a Battery Testing System (Neware Electronic Co., China). Cyclic voltammetry was performed using an electrochemistry workstation (CHI 760E, Shanghai), a voltage range between 0.01–3 V, and a scan rate of 0.2 mV s⁻¹.

S2. Supplementary figures

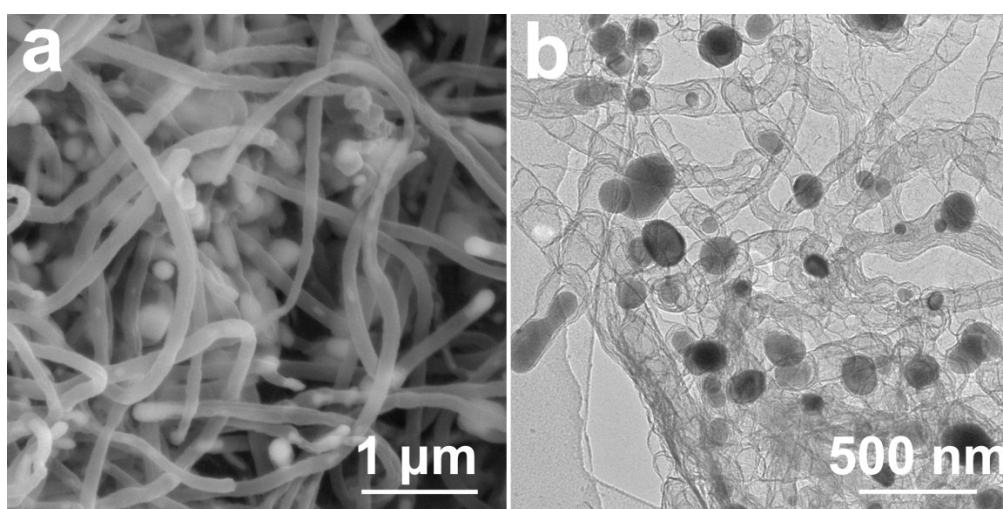


Fig. S1 SEM image (a) and TEM image (b) of Co@N-BCNTs@Co.

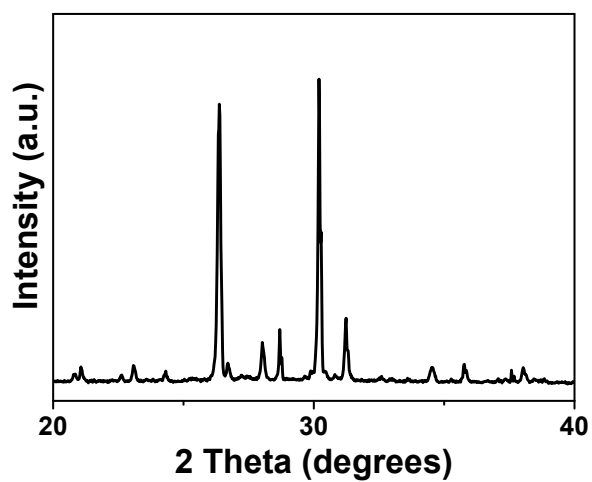


Fig. S2 XRD pattern of precursor (DCD+CoCl₂).

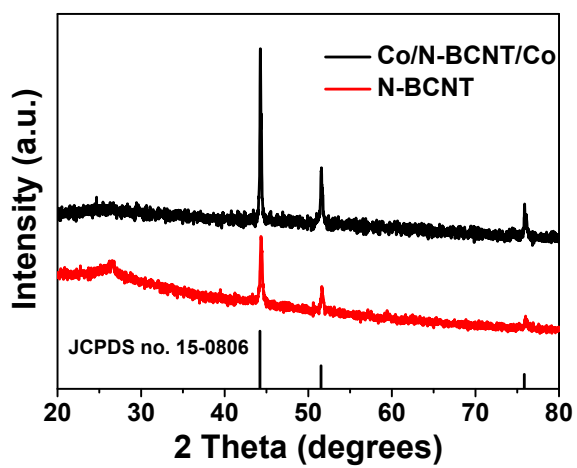


Fig. S3 XRD patterns of Co@N-BCNTs@Co and N-BCNTs.

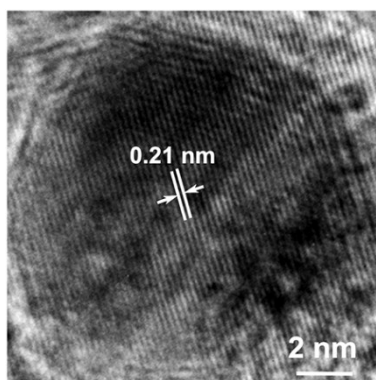


Fig. S4 HRTEM image of Co nanoparticle in the N-BCNTs.

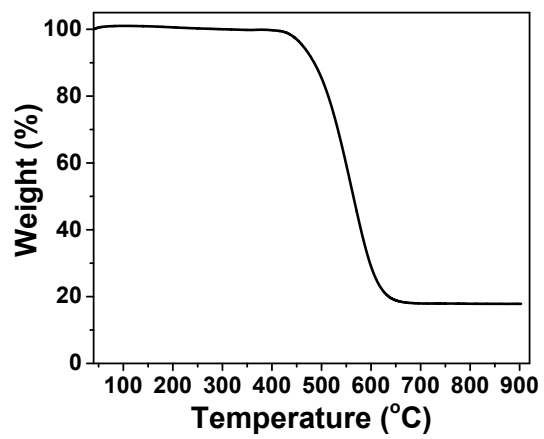


Fig. S5 TGA curve of N-BCNTs.

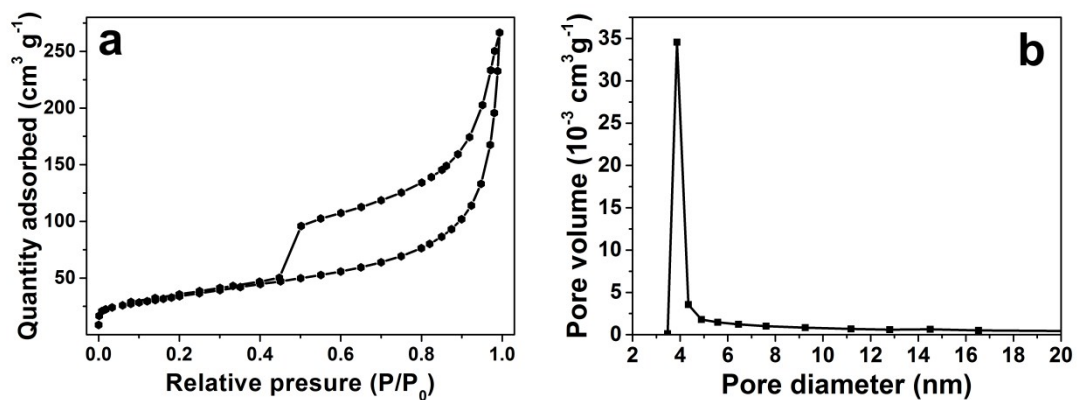


Fig. S6 (a) N₂ adsorption–desorption isotherms and (b) porosity distribution by BJH model of N-BCNTs.

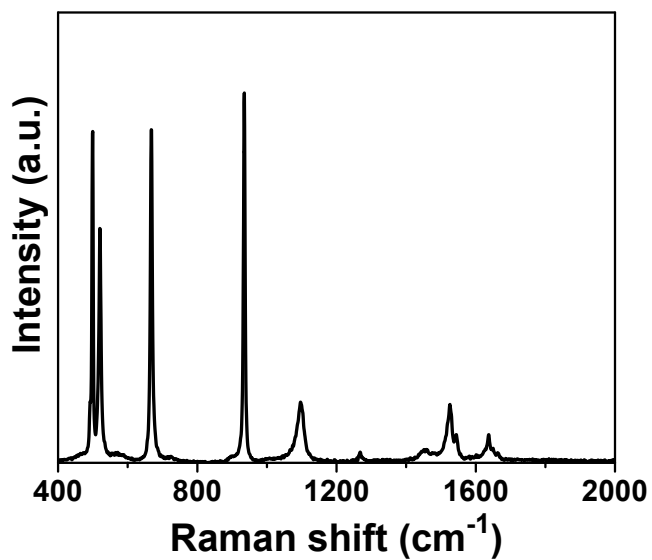


Fig. S7 Raman spectrum of precursor (DCD+CoCl₂).

Table S1 Element analysis of N-BCNTs

Samples	C	N	N:C
N-BCNTs-0.5 h	78.5	6.6	0.083
N-BCNTs-1 h	81.4	2.1	0.026
N-BCNTs-2 h	90.2	2.1	0.023

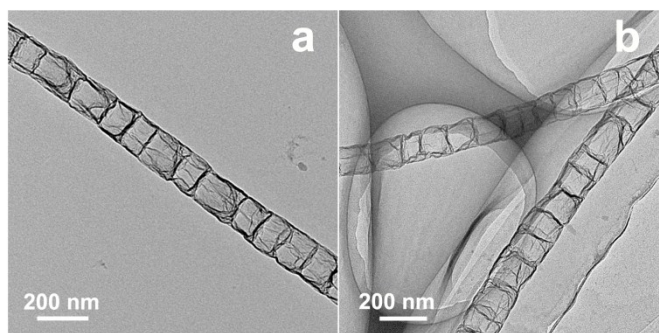


Fig. S8 TEM images of N-BCNTs at different pyrolysis times of 0.5 h (a) and 2 h (b).

S3. Lithium ion battery performance

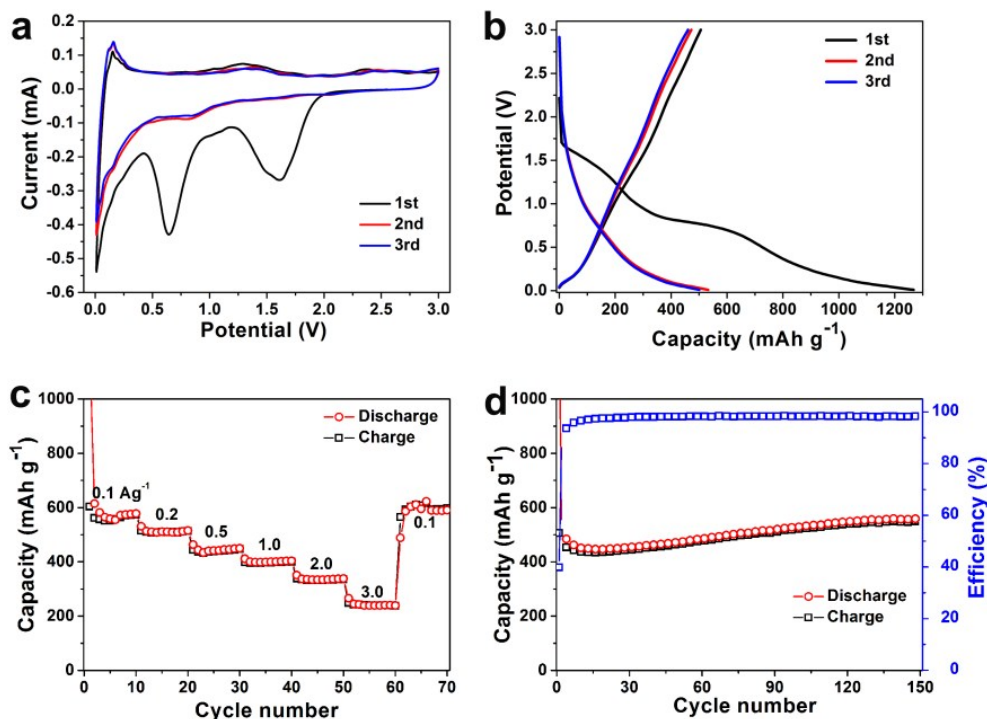


Fig. S9 (a) CV curves; (b) Discharge–charge profiles at a current density of 50 mA g⁻¹; (c) Cycle performance of N-BCNTs at various current densities of 0.1, 0.2, 0.5, 1.0, 2.0, 3.0 and 0.1 A g⁻¹; (d) Cycle performance of N-BCNTs at the current density of 0.5 A g⁻¹. All carried out in the voltage range 0.01–3.0 V vs. Li/Li⁺.

Fig. S9 displays the lithium-ion storage performance of the N-BCNTs electrode. The first three cycle curves of the CV are shown in Fig. S9a. During the first cathodic scan, N-BCNTs anode exhibits three cathodic peaks at approximately 1.7, 0.65 and 0V. The peak at 1.7V could be attributed to the reaction between lithium ions and a surface functional group, the peaks at 0.65 V are related to the formation of an SEI film, and the peak at 0V is ascribed to the insertion of lithium ions into the N-BCNTs. In subsequent cycles, the reduction peak at 1.7 and 0.65 V disappears. For the anodic scan, there is an obvious peak at 0.1 V which is attributed to the delithiation of N-BCNTs. From the second cycle onwards, the CV curves mostly overlap, indicating

good electrochemical reversibility. Figure S9b shows the initial three charge/discharge cycle curves of the N-BCNTs. The results agree well with the CV data. Fig. S9b shows the rate capability of N-BCNTs at various current densities from 0.1 to 3 A g⁻¹ and then back to 0.1 A g⁻¹, each for 10 cycles. The reversible capacities are 574, 514, 447, 400, 336, and 237 mA h g⁻¹ at 0.1, 0.2, 0.5, 1, 2 and 3 A g⁻¹, respectively. The rate performance of the N-BCNTs electrode is excellent when compared to other reports. Besides their superior rate capability, N-BCNTs also exhibit promising excellent cycle stability. Fig. S9d gives the cycling performance of the N-BCNTs electrode at a constant current density of 0.5 A g⁻¹. It is found that the reversible capacities show an upward trend with the cycles and reach 550 mA h g⁻¹ after 150 discharge/charge cycles. Meanwhile, the coulombic efficiency has been maintained at 98% after the 5th cycle, indicating the high lithium storage capability and excellent cycling stability of the N-BCNTs. Those superior lithium-ion storage performances of N-BCNTs anode could be attributed to the synergetic effect between its structure and instinctive high nitrogen content. More specifically, the hollow structure obtained herein could provide a large electrode/electrolyte interface and shorten the transport length of Li⁺, and the 1D structure benefit the electrochemical conduction of electrons, and the intrinsic nitrogen creates more Li⁺ storage sites and further enhances the electronic conductivity.